Investigation on Wireless Energy Harvesting Techniques for Internet of Things

Jiayi Huang *

United World College Thailand, Phuket, Thailand

* Corresponding Author Email: lydia_hjy08@163.com

Abstract. The Internet of Things (IoT), by collecting, processing, and uploading information from its surroundings, makes the preliminary base for the construction of a smart city. To utilize IoTs fully, establishing wireless sensor networks (WSNs) as a subset technology of the system is pivotal. Among all energy sources, the radio frequency energy, with its extensive coverage, easy accessibility, and characteristic of being free of spatial limitations, is the optimal choice for energy harvesting [1]. This project aims to conduct a thorough investigation on a wideband wireless energy harvester with high efficiency and verify its application prospect in portable power sources. I have comprehensively studied and modeled the components of a wireless energy harvesting system. I further fabricated the wireless energy harvester based on the optimized circuit diagram. It successfully featured a high sensitivity of 2701 V/W at 1.05 GHz or a wide bandwidth ranging from 0.5 GHz to 2.5 GHz. Finally, I used the devised sensor in real-life scenarios and successfully powered a thermos hygrometer and a LED. I built a network of multiple energy harvesters with an in-situ monitoring system, analogous to the IoT. In this work, I have proposed a methodology to fabricate wireless energy harvesters with high sensitivity and wide bandwidth. This research will bridge the gap between the scientific exploration for novel devices and their application in real-life scenarios.

Keywords: Internet of things, Wireless energy harvesting, Wireless sensor network.

1. Introduction

1.1. Contextual Background

The steadily increasing human population of 8.2 billion comes with significant demand and consumption for resources. Renewable, sustainable energy sources that can supplement and slowly replace the greenhouse-gas-generating fossil fuels are an essential issue for humans to tackle. Out of concern for the environment and the energy transition that is happening on a global scale, I decided to carry out this work on wireless energy harvesters that harvest ambient radio-frequency energy. Wireless sensors, nodes in the Internet of Things (IoT) that are not connected by wires are in charge of collecting, processing, and uploading information collected from their surroundings to build an entire information base that is the preliminary base for constructing a smart city. Wireless sensors have a wide range of real-life application possibilities, from smart cities and smart homes to operating in surgeries and engaging in medical treatments for patients.

To utilize IoTs fully, establishing wireless sensor networks (WSNs) as a subset technology of the system is pivotal. A sensor network covering entire cities consists of individually working nodes of great numbers and scattered locations; therefore, a stable energy source is necessary to sustain the network. Traditional batteries are passed as solutions as they are short-lived and expensive to replace. As an alternative, ambient energy harvesting technology, which collects scattered energy in the environment, with its energy type varying from solar power and wind power to vibration energy, is comparatively more sustainable in remote areas where constant recharge is hard to attain.

The correct energy source is a significant aspect of the issue. Among all energy sources, the radio frequency (RF) energy harvesting technology, with its extensive coverage, easy accessibility, and characteristic of being free of spatial limitation on the receiving node and energy dissipation in wires, makes it the optimal choice for charging nodes requiring small power (its passing current ranges from 500nA to 100mA).

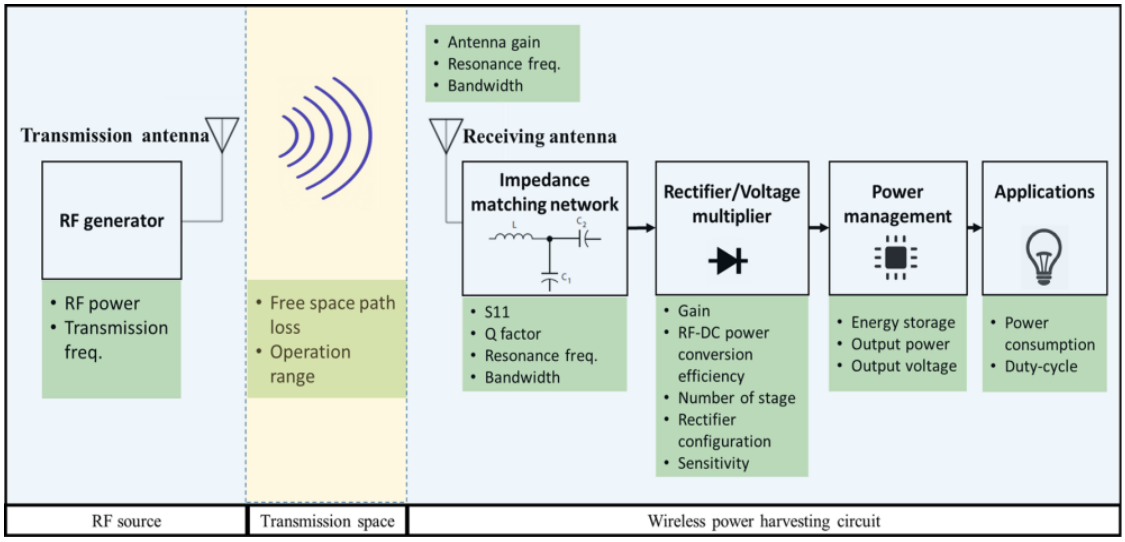

Figure 1. Conceptual block diagram of an RF power harvesting system

1.2. Literature Review

In current studies, researchers have focused on three approaches to improving the performance of wireless energy harvesting technology: modifying the structures of the antenna, matching network, or rectifier circuit.

Hichem Mahfoudi and his team's work on the geometry of the antenna resulted in the introduction of a wideband fractal slotted ground plane antenna with a dual-linear polarization, an iterative model, in their essay "A Wideband Fractal Rectenna for Energy Harvesting Applications" [2]. This antenna, designed and optimized to operate between 1.5 and 2.65 GHz, achieved an impressive 70 percent efficiency, demonstrating the practical value of their research. Similarly, Sunanda Joy and her team's work on the geometry of the antenna [3] also led to the suggestion of a two-armed self-complementary log-periodic frequency-independent toothed planar multiband antenna with twelve radiators in a separate port and annular ring shape. This antenna achieved a maximum DC rectification efficiency of about 52 percent for negative 20 dBm input RF power from 0.9 GHz to 2.6 GHz.

Moving on, matching networks play an essential role in impedance matching, hence being able to mitigate RF energy loss along transmission. Most matching circuits are single-component diodes, employing diodes such as the HSMS2860 Schottky diode [4]. In "Two-dimensional MoS2-enabled flexible rectenna for Wi-Fi-band wireless energy harvesting", a novel two-dimensional material, MOS2, has been incorporated into developing a Schottky diode with better performance [5]. The system's maximum power efficiency is 40.1 percent when an input power of 0.7dBm is provided. Several researchers presented designs that can be characterized as broadband. Mohamed M. Mansour and his team's rectifier design improved performance through their effort to limit the number of components. Interestingly, they replaced conventional diodes that function as matching networks with L-shaped defects on the ground plane. Their model, in practice, achieved a max of 59.5 percent efficiency at 2.45GHz.

The rectifier circuit plays a determining role in the output voltage level and has subsequently received much attention in research. One attempt from Joydeep Banerjee and Subhasish Banerjee was to combine a Wilkinson power combiner with a conventional voltage multiplier [6].

Concluding from current studies on wireless energy harvesting technology, three major research gaps exist.

First, most current wireless energy harvesters can only work in a narrow bandwidth due to the notable impedance variations in frequencies. In contrast, ambient wireless radiation expands over a wide frequency range from tens of MHz to several GHz. Developing wideband energy harvesters that can work over two or more frequency bands is of great importance for real applications.

Secondly, the demand for high sensitivity and high energy conversion efficiency has yet to be fulfilled. The power for ambient wireless radiation is typically very low (orders of micro-Watt or

nano Watt). The sensitivity of wireless energy harvesters should be sufficiently high (orders of several thousand V/W or higher) to meet the voltage requirements of electric appliances.

Thirdly, although wireless energy harvesters have been extensively studied in laboratories, reports of their application in real-life scenarios are very rare. Pioneering research on the application of wireless power sources for electric devices and sensors is urgently needed.

The rectifier circuit plays a determining role in the output voltage level and has subsequently received much attention in research. One attempt from Joydeep Banerjee and Subhasish Banerjee was to combine a Wilkinson power combiner with a conventional voltage multiplier [6].

1.3. Section Overview

In this work, I will thoroughly investigate a wide band wireless energy harvester with high efficiency and verify its application prospect. In section two of this paper, I will introduce the theory and operating mechanism behind each of the components of a wireless energy harvesting system. In section 3, the design and optimization of the circuit performance process using Matlab and RFSim99 is explained and documented in detail. In section 4, I will report the fabrication of the energy harvesters and their responsiveness to different frequencies of RF energy in the laboratory environment. In section 5, I will present the performance of the devised sensor in real-life scenarios and extend its potential application in the Internet of Things. My research may bridge the gap between scientific explorations and applications, pushing forward wireless energy harvester's application in real-life scenarios.

2. Theoretical Background

Because the wireless energy harvester system works on RF range, the design of the transmission line connecting all different components should be carefully thought through: the antenna, the impedance matching network, the rectifier circuit, and the power management unit. Here, I will briefly discuss the theories on designing these components.

2.1. Transmission Line

Different types of microwave transmission lines, such as coaxial cable, coplanar waveguide, and microstrip, are used to efficiently deliver microwave currents. The microstrip is particularly suitable for compact circuit applications because of its high compatibility with printable circuit board (PCB) technology. In a microstrip transmission line, there is the ground plane, dielectric substrate, and the signal line. The ground plane's existence played a major role in suppressing the radiative loss by limiting the electric field to the ambient of the signal line. The relative dielectric constant measures the ability of dielectric substrate, opposite to conductors, to store electrical charges. It is related to the intensity of the electric field in the dielectric substrate. The transmission line is sandwiched by air and the dielectric substrate, and the effective relative dielectric constant can be expressed as:

$$\epsilon_{re} = \frac{\epsilon_r+1}{2} + \frac{\epsilon_r-1}{2}[(2 + \frac{12h}{w})^{-\frac{1}{2}}] + 0.041(1 - \frac{W}{h})^2 \quad (1)$$

Where epsilon r is the relative dielectric constant of the substrate, w is the width of the microstrip line and h is the height of the microstrip line. The above equation works when the width is smaller or equal in value compared to the microstrip's height. When the width is greater or equal in value compared to the microstrip's height, the following equation is used.

$$\epsilon_{re} = \frac{\epsilon_r+1}{2} + \frac{\epsilon_r-1}{2}(1 + 12\frac{h}{W})^{-\frac{1}{2}} \quad (2)$$

The impedance of the transmission line can thus be calculated through the following equation when width is smaller or equal in value compared to the microstrip's height.

$$Z_0 = \frac{60}{\sqrt{\epsilon_{re}}} In\ (\frac{8h}{W} + \frac{W}{4h})\Omega \tag{3}$$

The following equation should be used if the width is greater or equal in value compared to the microstrip's height.

$$Z_0 = \frac{120\pi}{\sqrt{\epsilon_{re}}[\frac{W}{h}+1.393+0.667In\ (\frac{W}{h}+1.444)]}\Omega \tag{4}$$

In order to match the impedance of the transmission line, the dimension of the transmission line can thereby be able to be calculated. The following equation works when the ratio between the width and height is smaller or equal to 2.

$$\frac{W}{h} = \frac{8e^A}{e^{2A}-2} \tag{5}$$

On the other hand, when the ratio is greater or equal to 2, the following equation works.

$$\frac{W}{h} = \frac{2}{\pi}\left\{B - 1 - I\ n(2B-1) + \frac{\epsilon_r - 1}{2\epsilon_r}\left[I\ n(B-1) + 0.39 - \frac{0.61}{\epsilon_r}\right]\right\} \tag{6}$$

In the above two equations, the A and B could be calculated with the following equations.

2.2. Antenna

$$A = \frac{Z_0}{60}\sqrt{\frac{\epsilon_r+1}{2}} + \frac{\epsilon_r-1}{\epsilon_r+1}(0.23 + \frac{0.11}{\epsilon_r}) \tag{7}$$

$$B = \frac{377\pi}{2Z_0\sqrt{\epsilon_r}} \tag{8}$$

When choosing the suitable antenna, we need to pay attention to four attributes: the first two are the field pattern and power pattern. Both patterns would have a major lobe and a minor lobe; in the field pattern, the major lobe's direction is the directivity. Another trait we should pay attention to is the half-power beam width. It is the width of the lobe when its power or field intensity drops to half of the maximum intensity. A bigger half-power beamwidth marks a greater emission angle, and a smaller one marks better directivity. The two other attributes are gain and the reflection coefficient. The gain is the radiation power divided by the input power, thereby no greater than one. The reflection coefficient includes the input or output impedance (though they are equivalent since the antenna is a resistive element, and the reference impedance (usually 50 ohms). To select a suitable antenna, we have simulated the performance of different types of antennas using Matlab.

The two types of antennas I simulated in Matlab are microstrip antennas and Yagi-Uda antennas. In theory, Yagi-Uda antennas have wide bandwidth and low directivity. On the other hand, microstrip antennas have high directivity, narrow bandwidth, and high compatibility with PCB technology as they are usually thin and lightweight.

2.3. Rectifier Circuit

To achieve the goal of turning alternating current into direct current, one of the most preliminary methods is to use a diode to construct half-wave rectification. Only half of the entire cycle could pass through, causing the loss of half of the current.

2.3.1. Bridge Rectifier.

Bridge rectifier is a type of full-wave rectification, arranging four or more diodes in a circular formation. Though both the positive and negative half cycles will be output, the max voltage remains the same before and after rectifying, resulting in low power.

2.3.2. Dickson Charge Pump. A charge pump is the solution to the flaws of the previous rectifiers: it could achieve a significant increase in output voltage.

A Dickson charge pump is formed of various loops of capacitors and diodes. With currents of alternating charge at the two ends, diodes could carry the voltage along the path and accumulate voltage at each capacitor as current constantly travels in alternating direction.

When Vrf is the positive side with a voltage of U, the current passes through C1, D2, and C2. Then, GND becomes the positive side. The current passes through D1 and C1, and charges the right side of C1 with one U of voltage (the right side is now positive). Once again, the Vrf is the positive side, the current charges the left side of C1 with 1U and the right charge, since it is one U higher in voltage compared to the left side, it now has a voltage of 2U (and the net voltage of C1 is U). The 2U would also be carried to C2, resulting in C2 carrying a voltage of 2U. It works similarly in other capacitor and diode loops, achieving an arithmetic increase in voltage.

In the Dickson charge pump, the end voltage is proportional to the number of stages contained, with each stage containing an additional capacitor and diode.

$$V_n = 2N(V_i - V_t) \tag{9}$$

In the above equation, Vin is the maximum input voltage, Vth is the threshold voltage for the diode.

In order to proceed on the circuit simulation using RFSim99, we need to convert the impedance of the diode into resistance. By reading the instructions of HSMS-282x, I was able to obtain the equivalent circuit to represent the diode.

Linear Equivalent Circuit Model
Diode Chip

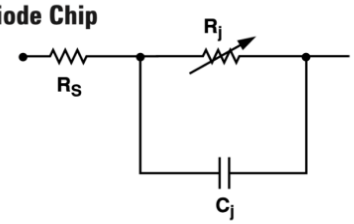

R_S = series resistance (see Table of SPICE parameters)

C_j = junction capacitance (see Table of SPICE parameters)

$$R_j = \frac{8.33 \times 10^{-5}\ nT}{I_b + I_s}$$

where
I_b = externally applied bias current in amps
I_s = saturation current (see table of SPICE parameters)
T = temperature, °K
n = ideality factor (see table of SPICE parameters)

Note:
To effectively model the packaged HSMS-282x product, please refer to Application Note AN1124.

SPICE Parameters

Parameter	Units	HSMS-282x
B_V	V	15
C_{J0}	pF	0.7
E_G	eV	0.69
I_{BV}	A	1E-4
I_S	A	2.2E-8
N		1.08
R_S	Ω	6.0
P_B	V	0.65
P_T		2
M		0.5

Figure 2. Equivalent circuit model of HSMS-282x

2.4. Matching Network

Impedance matching networks are necessary since the input impedance of the initial power supply is usually inequivalent to the impedance of the load's impedance. The output power of the circuit reaches its max when the two impedances (active resistance) are equivalent. For complex impedance, other than having the active resistance being equivalent, the reactance needs to be conjugate reactances to have maximum power.

Other than maximizing the power of the circuit, impedance matching is also important to avoid damaging the circuit. We could measure the energy being reflected through the reflection coefficient, which is the impedance of the load minus the standard resistance (usually 50 ohms) over the impedance of the load plus the standard resistance. On top of the reflection coefficient, we get the

voltage standing wave ratio, which measures the intensity of the standing wave created by the reflected energy.

When matching impedance, we could use the smith chart to figure out the type of circuit component required and the impedance required.

In matching networks, a low-pass filter can be used to match the impedance between the source and the load, particularly when dealing with low-frequency signals, while high-pass filters are for high-frequency signals. By rearranging capacitors and inductors, we could create either high-pass or low-pass filters.

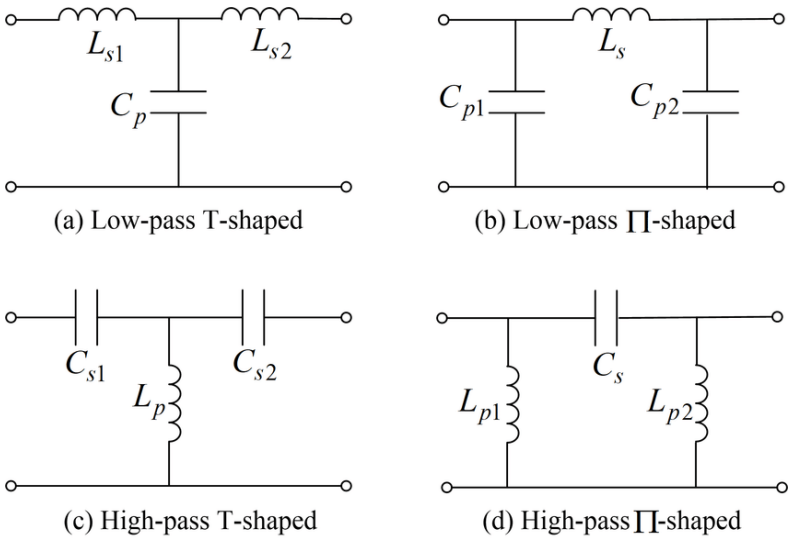

Figure 3. Different types of low-pass and high-pass filters

2.5. Power Management Unit

My designed energy harvesting system is prepared for charging appliances and offering electrical energy to other electronic components. In this circuit, I utilize the power management unit as a switch between “sleep mode”: long-term low-power to “active mode”: short-term high-power.

In this experiment, I chose to use PW5103. Compared to other management chips in the market, PW5103 has a low minimum input voltage requirement 0.7V and high laboratory efficiency 95 percent. In the simulation, the equivalent circuit for a PW5103 has been located and used.

3. Design Simulation

3.1. Transmission Line Design

When designing the transmission line, the goal is to match its impedance to 50 ohms, which is the impedance of electronic components. I have simulated the impedance of strip lines using the TX line software.

The calculated parameters are shown below.

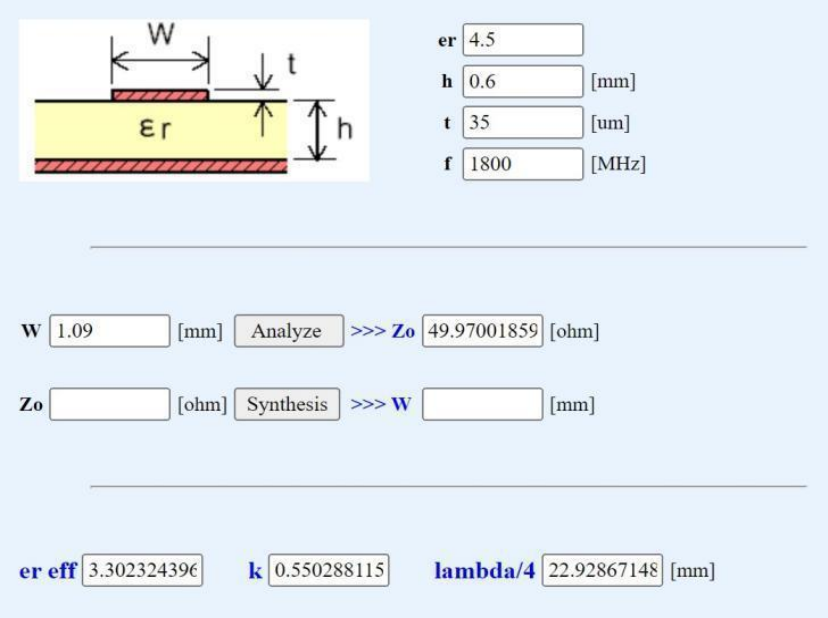

Figure 4. Parameters of the strip line

In the calculations, the FR4 (relative dielectric constant of 4.5) substrate is chosen. The calculated line width and substrate thickness are 1.09 mm and 0.6 mm, respectively. The calculation also indicates that the impedance is around 50 ohms in the frequency range between 1 to 2 GHz.

3.2. Antenna Design

In antenna design, we are looking at the directivity and S11 of the antenna. Directivity is how concentrated the radiation of the antenna is in certain directions, and it is calculated by the ratio and the maximum and average RF power density at a certain direction. S11 represents the one-port RF reflectivity. A smaller value of RF reflectivity means more power to be transmitted by the antenna.

I have compared the performance of a strip line antenna and an Uda antenna using Matlab simulations. The strip line simulation shows that the max directivity of this antenna is 10.1 dbi. The S11 curve represents a minimum power reflectivity of -22.3 dB at 2.4 GHz.

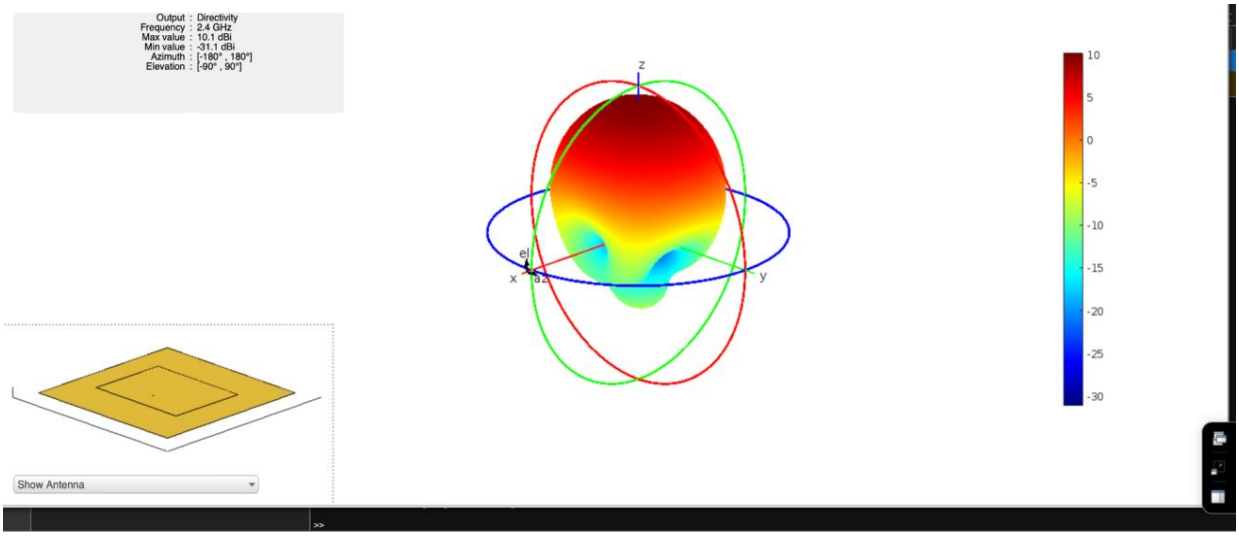

Figure 5. Directivity of the strip line antenna

The Uda line simulation shows that the max directivity of the Uda antenna is 10.2 dbi. The S11 curve represents a minimum power reflectivity of -5.5 dB at 2.4 GHz.

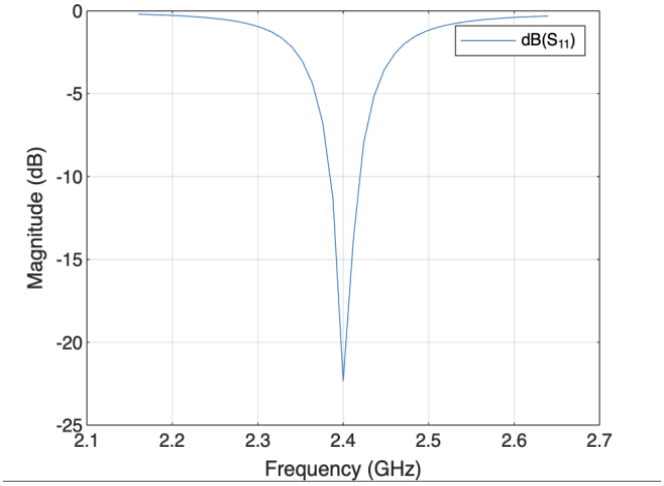

Figure 6. S11 of the Strip line antenna

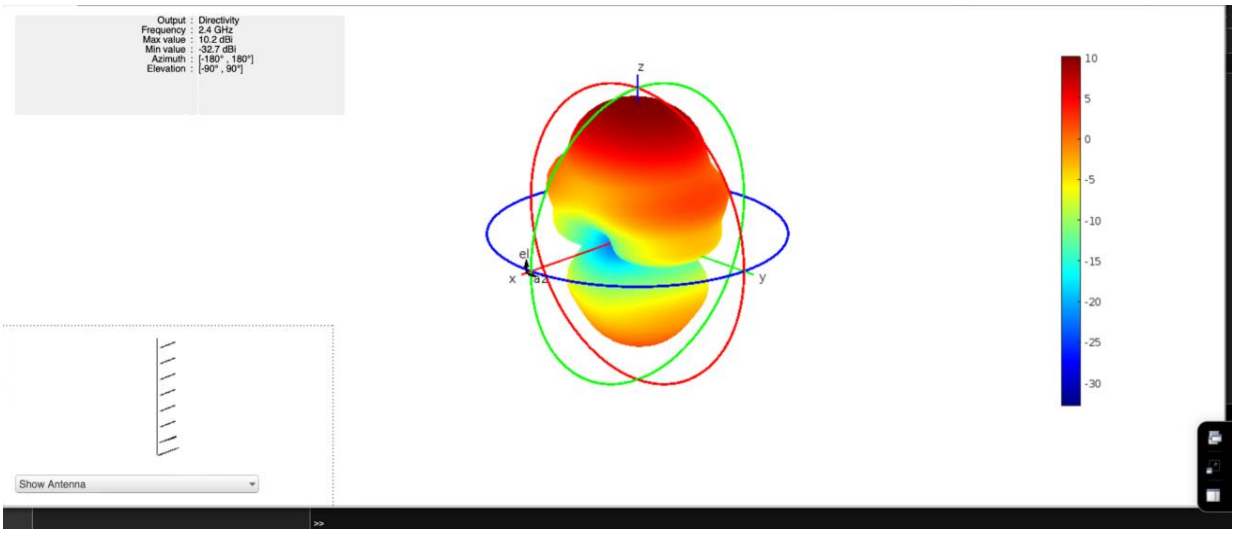

Figure 7. S11 of the Uda line antenna

The comparison of the two sets of data led to the conclusion that a strip line antenna has better overall performance (lower directivity). Meanwhile, it is compatible with the printed circuit board technology. Therefore, it is more suitable for wireless energy harvesting to use strip line antennas. On the other hand, the Uda antenna has a broader frequency bandwidth of 0.15 GHz, which is advantageous for broadband energy harvesting.

3.3. Circuit Impedance Matching

A four-stage charge pump is selected for RF rectification. The charge pump circuit is composed of four Schottky diode chips (HSMS 285C) and four capacitors. To match the impedance of the rectifier to 50 ohms, a pi-type matching circuit is used. The circuit diagram is shown in figure 8.

In this circuit, P1 is a SMA interface that is used for connecting an antenna. CM1 is the DC blocking circuit that protects other electronic components from DC current existent in the circuit. CM2, CM3, and LM1 are composers of the PI match circuit. C1 to C4 and Q1 to Q2 makes up the four-stage charge pump. DC out 1 leads the output voltage of the circuit to the power management circuit. PW5103 is the power management unit. I have built the equivalent circuit for the Schottky diodes and simulated the circuit using RFsim99 (fig. 8). Based on the automatic impedance matching, the recommended values for CM1, LM1 and LM2 can be obtained. The simulated Smith Chart also reveals impedance numbers close to 50 ohms in the range of 2.3 to 2.5 GHz.

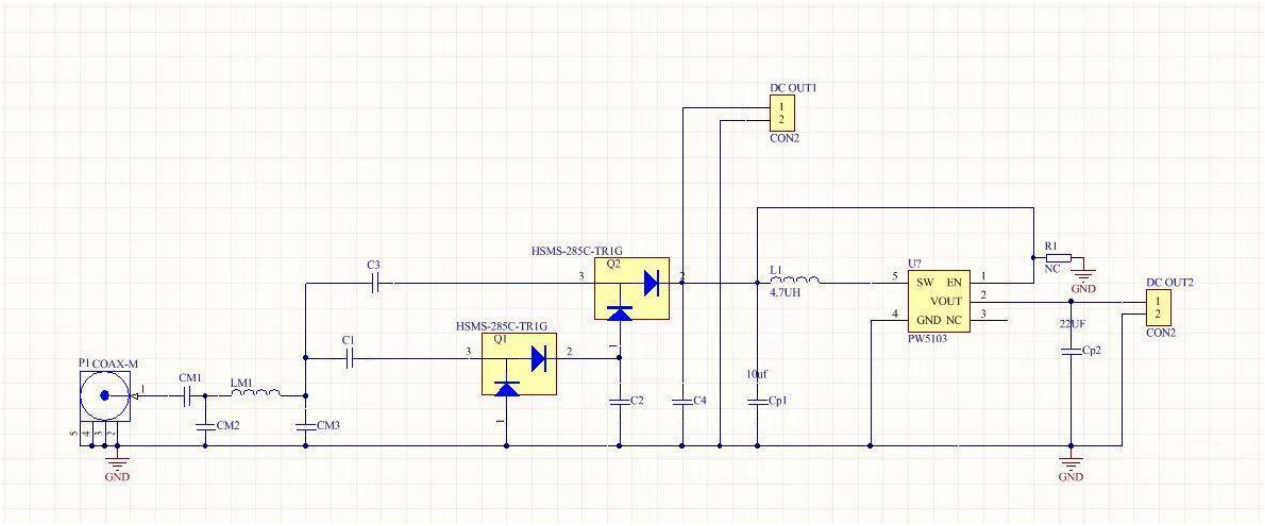

Figure 8. Design of the wireless energy harvester

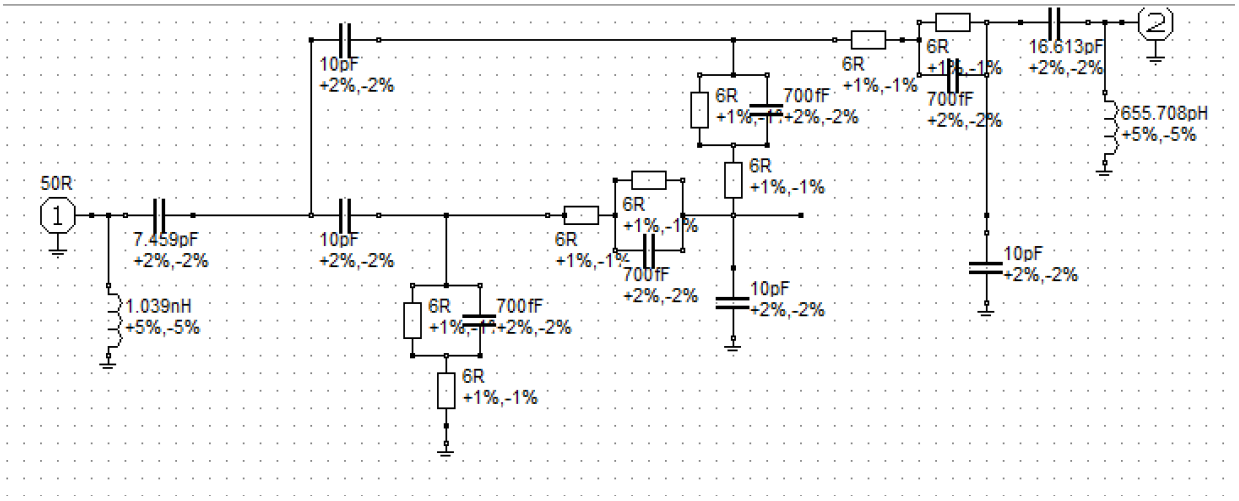

Figure 9. Simulation with equivalent networks in RFsim99

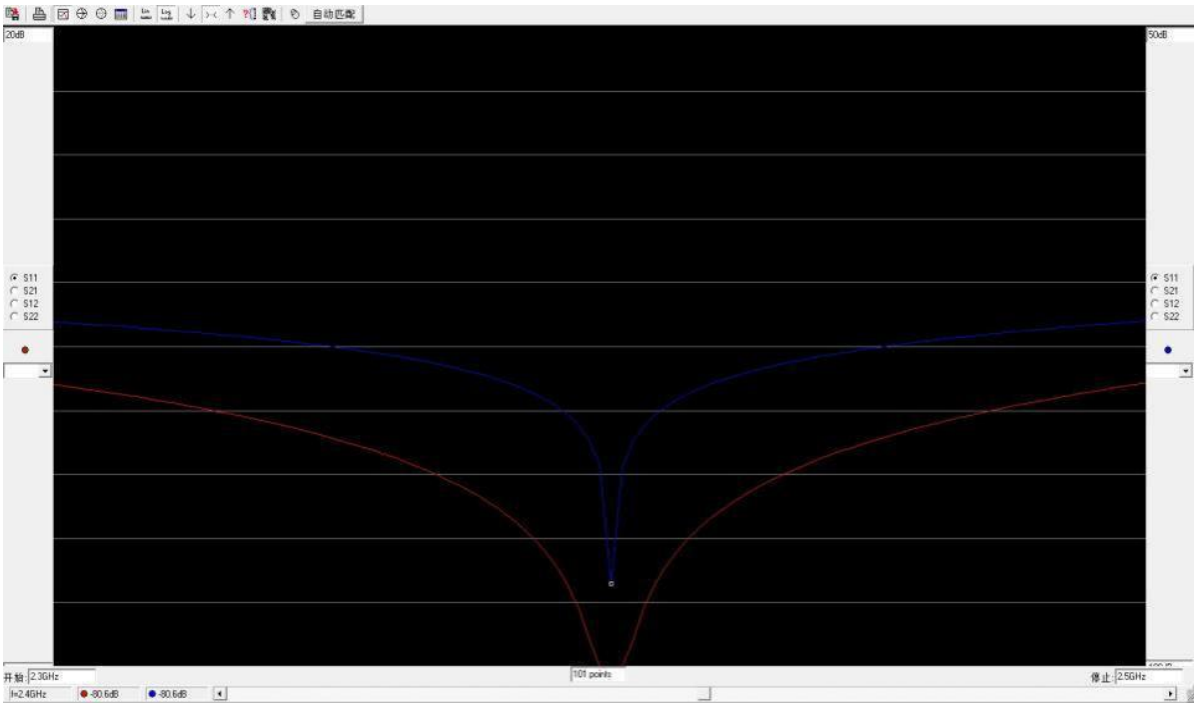

Figure 10. S11 curve of the designed circuit

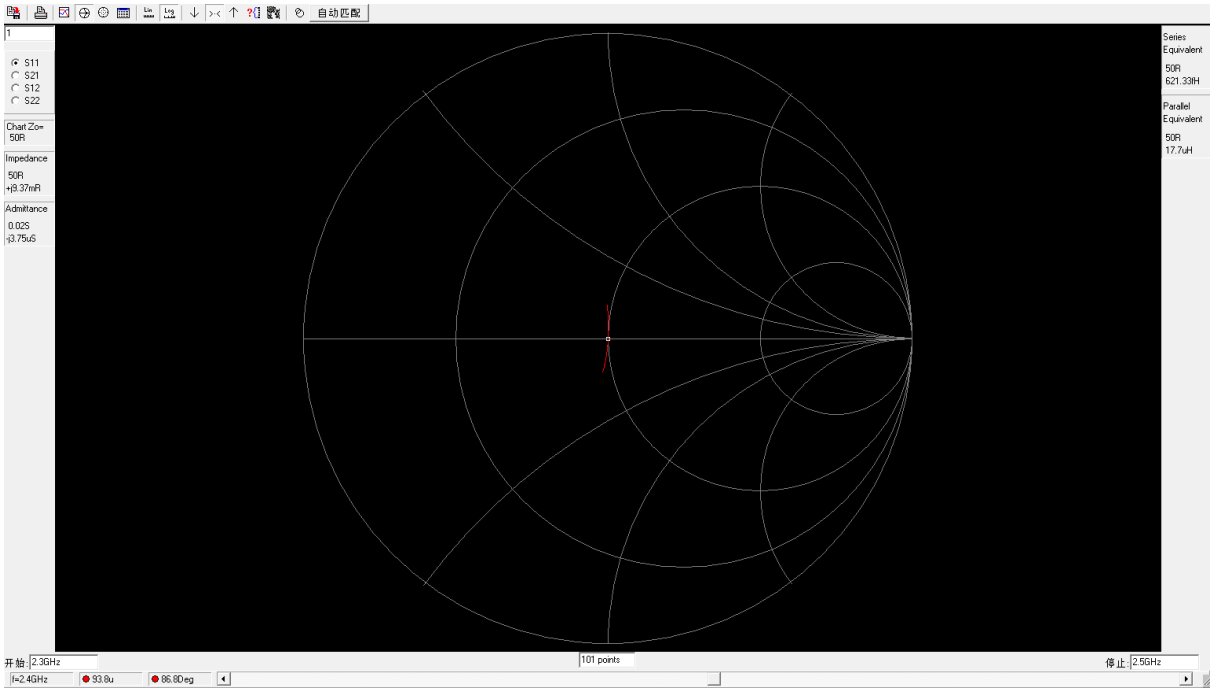

Figure 11. Smith Chart of the designed circuit

4. Experimental Implementation

4.1. Energy Harvester Construction

I have drawn the PCB layout of the designed circuit diagram (figure 11). The PCB board was fabricated based on the simulated parameters. To be specific, a double layer PCB technology is used. The substrate is FR4 that is 0.6 mm thick. The thickness for the copper layer is 35 mm. The width of the strip line is 1.09 mm.

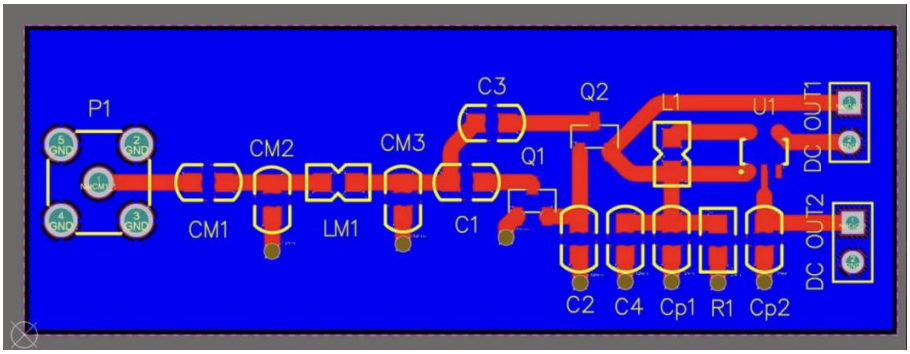

Figure 12. Drawn PCB Layout

I have mounted the electric components onto the PCB board using hot air gun wielding. During the mounting process, extra attention must be paid to avoid fake wielding. I used a multimeter to ensure that electrical components are fully wielded. A photograph of the wielded PCB is figure 15. P1 is connected to a SMA jack for connecting the antenna. DC Out 1 and 2 are output pins from the charge pump and the power management unit.

Figure 13. Picture of welding equipment

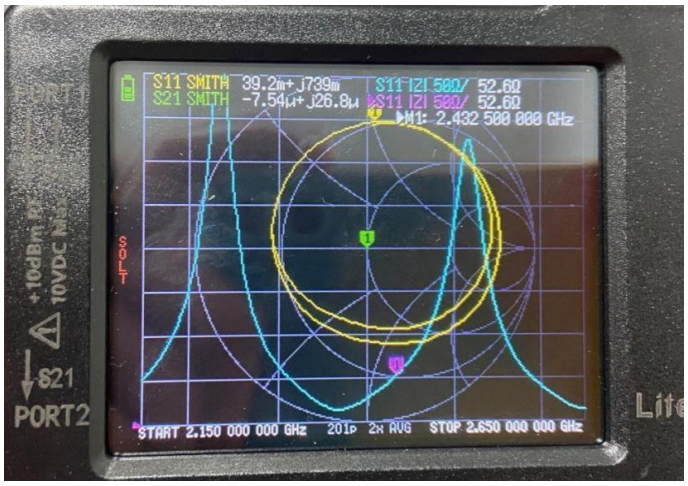

Figure 14. Picture of a Smith Chart on the network analyzer

I have measured the input impedance of the circuit from P1 with a portable network analyzer. By observing the position of the complex conductance in the Smith chart (Figure 14), I can easily match the impedance to 50 ohms through changing the values of matching circuits. In general, the arcs represent different reactances and a horizontal axis represents a value of resistance. To move the point that represents the current value to a higher position in the arc, connect an inductor in series; for opposite effect, connect a capacitor in series. To move the point to a more distant point in the arc from the center, connect an inductor in parallel; for opposite effect, connect a capacitor in parallel. I have further replaced the impedance matching components in order to reach a 50 ohms impedance over the frequency range.

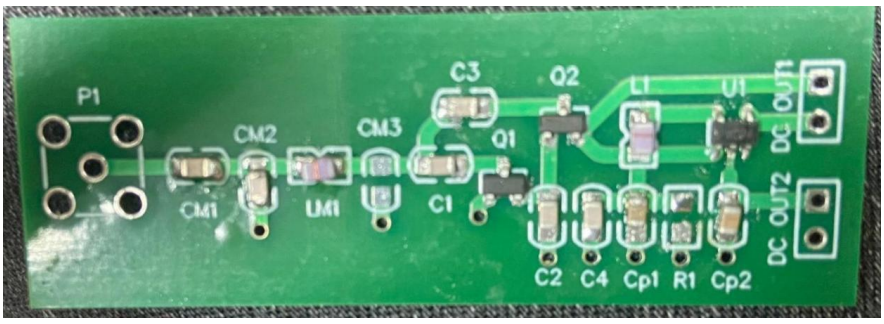

Figure 15. Picture of the energy harvester with mounted electrical components

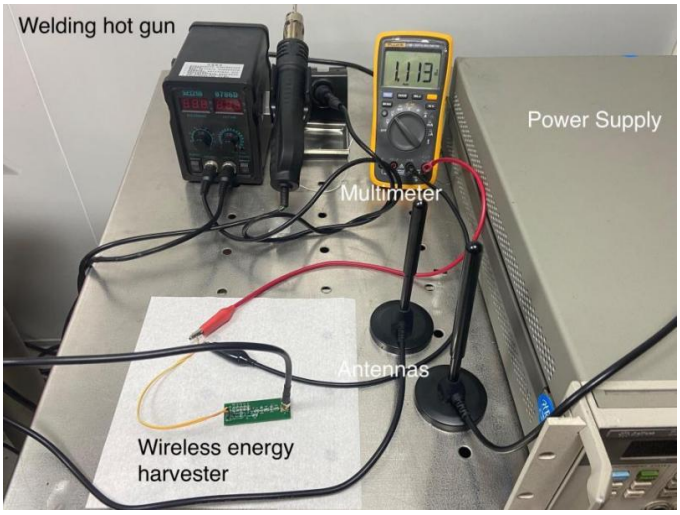

Figure 16. Voltage monitoring of the circuit

Initially, CM1 is a 10 pF capacitor, CM2 is a 7.5 pF capacitor, LM1 is a 1nH inductor, C1 to C4 are 10pF capacitors，Q1 and Q2 are HSMS285C-TR1G, L1 is a 5uF capacitor, CP1 is a 10uF capacitor, CP2 is a 22uF capacitor, namely sample 1. The spectral response of this wireless energy harvester is shown in figure 17. It is evident that the energy harvester exhibits a maximum DC output at around 1.05 GHz. The maximum sensitivity is 2701 V/W, which far exceeds the sensitivity of a single Schottky diode (20 V/W). I also measured the power dependence of the energy harvester, and observed an increase in output voltage with RF power. Such a device is suitable for working at frequencies ranging from 1 to 1.1 GHz. However, it doesn't match well with the working frequency of cellular communications or WIFI. So, I further modified the working frequency of the energy harvester through changing the impedance matching circuit.

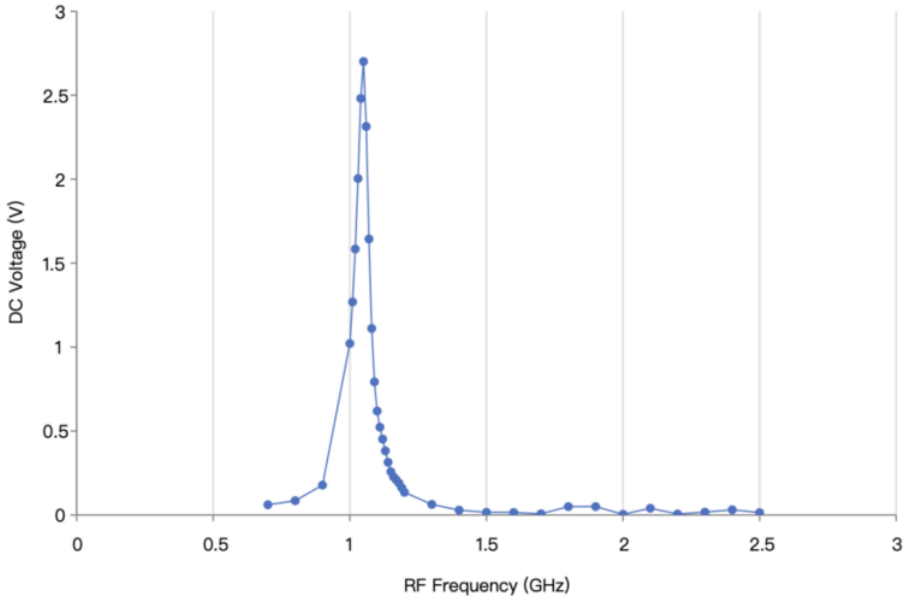

Figure 17. Spectral response of the wireless energy harvester sample 1 to RF frequency

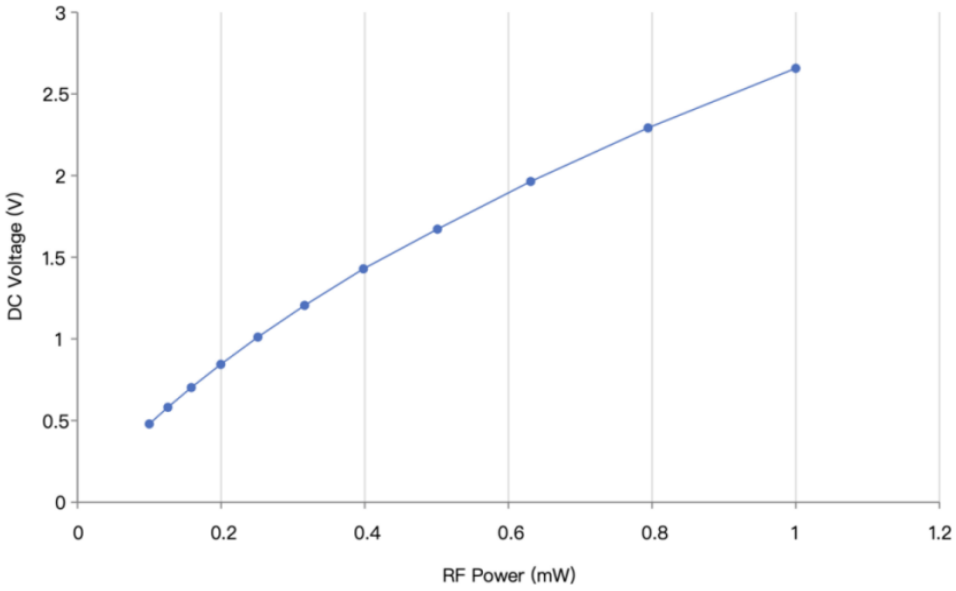

Figure 18. Power dependence of the wireless energy harvester sample 1

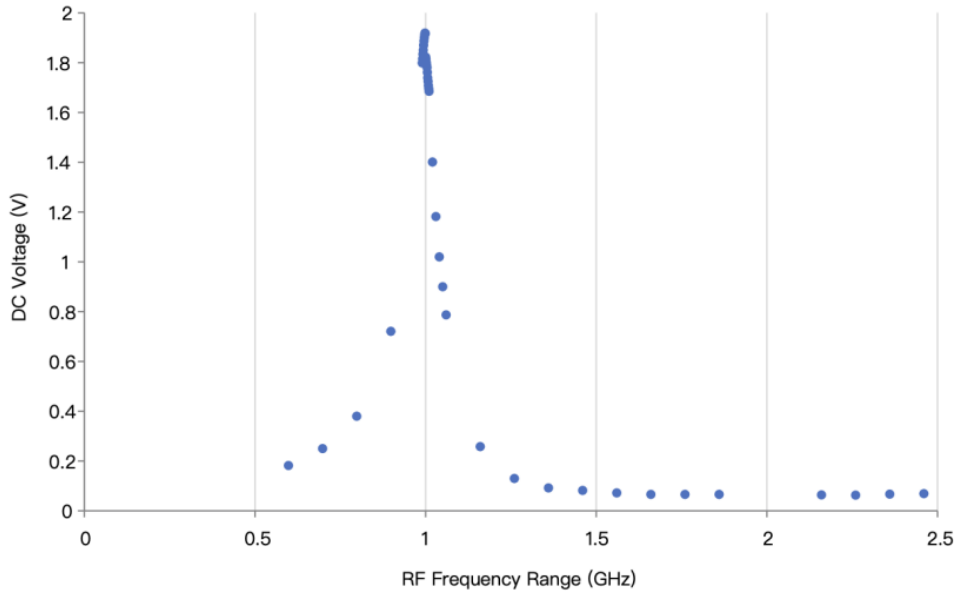

Figure 19. Spectral response of the wireless energy harvester sample 2 to RF frequency

After changing the values of C1, C2, and C4 to 5pF, C3 into a HSMS2822 diode, L1 to 3.3nH, the peak frequency is reduced to 1 GHz, getting closer to the 2G cellular frequency of 0.8 to 0.9 GHz, which is sample 2. Therefore, I made further adjustments to sample 2 by taking away the capacitor on C2 and putting a 1 nF capacitor at CM1.

For sample 3, the working frequency covers a wide frequency range between 0.5 GHZ to 0.9GHZ, suitable for harvesting 2G wireless signals. More intriguingly, a new peak emerges between 2.1 to 2.5 GHz in the spectral response curve. This character indicates that it can also harvest WIFI signals. We can conclude that the wireless energy harvester has a dual-band feature. It has application prospects for wireless energy harvesting in indoors and outdoors conditions.

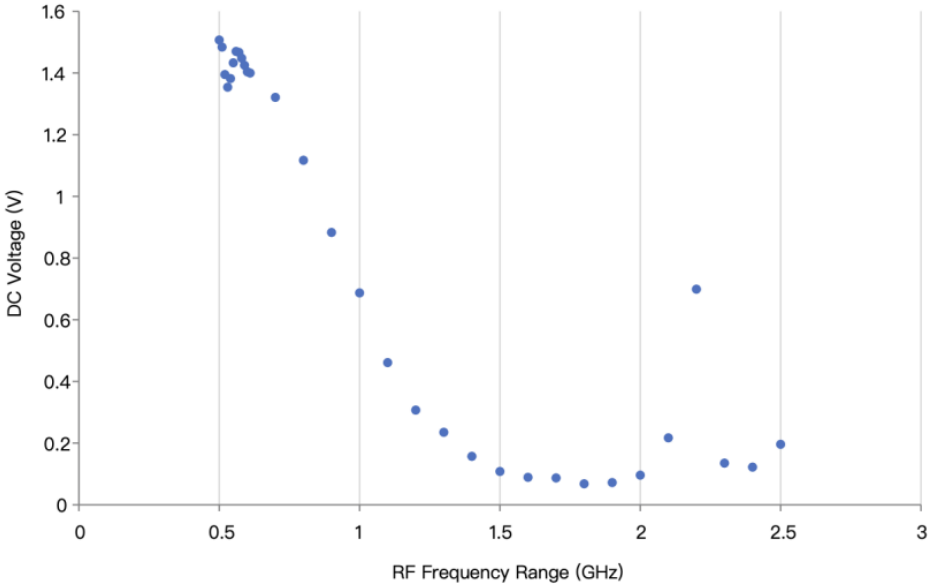

Figure 20. Spectral response of the wireless energy harvester sample 3 to RF frequency

5. Application

Based on the prominent performance of the energy harvesters, I have explored its application in real life scenarios. As a proof of concept, I have used the output of the energy harvester to power a red light-emitting diode (LED). The input of the energy harvester is connected to an antenna with -5 dbi gain and frequency range of -700~2700 GHz. As shown in figure 22, the LED can be lit up with the energy supplied for the wireless energy harvester. This success proves its potential in powering low-power electronic devices. I then attach it to a thermo hygrometer as a replacement for a battery (fig. 22). The proper functioning of the thermo hygrometer implied the feasibility of using my wireless energy harvester to power other electronics and its potential in wireless sensor networks used in a wide range of industries.

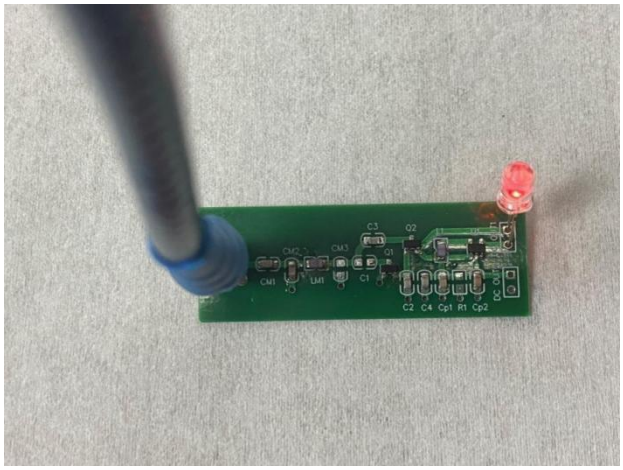

Figure 21. Powering a light using the wireless energy harvester sample

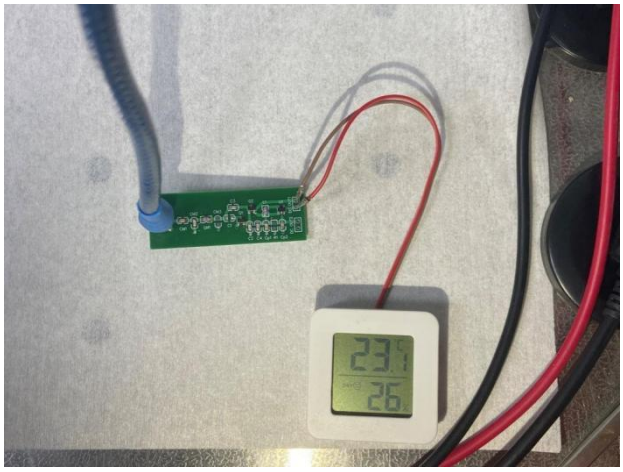

Figure 22. Powering a thermo hygrometer using the wireless energy harvester sample

All in all, my wireless energy harvester has proven its capability to replace traditional batteries as an energy source to charge electronics.

5.1. In Situ Monitoring of Wireless Energy Harvesting Network

In applying Internet of things or wireless sensor networks, I need close monitoring of the up-to-date working status of the distributed nodes. To meet this demand, I have built a wireless voltage sensor network that can monitor multiple wireless energy harvesters at the same time. For testing, I have placed three monitors in three separate locations.

I have also developed a user interface for real time display of the output voltage of wireless harvester networks using Labview software (as shown in figure 23). Such a system pioneered the prospect of application of wireless information communications.

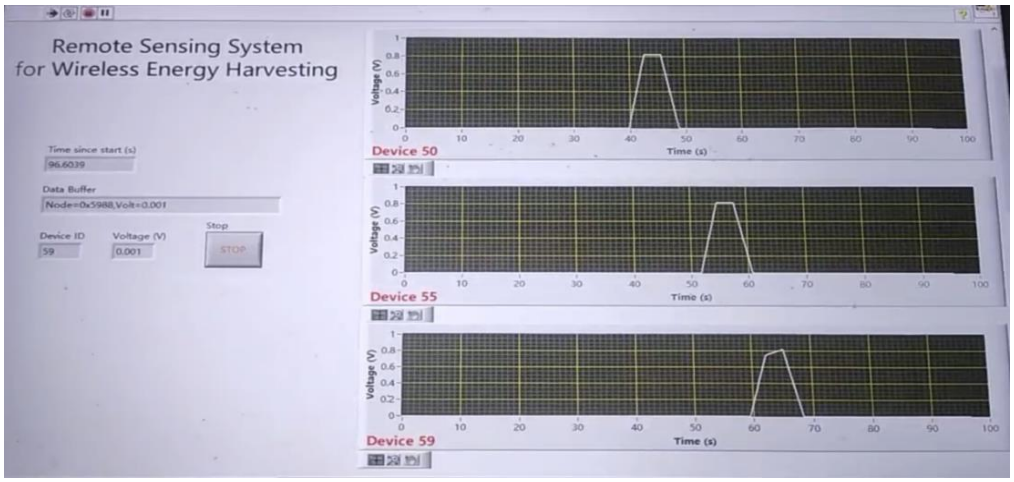

Figure 23. User interface of the monitoring program

6. Conclusion

In summary, I have designed and constructed wireless energy harvester. I have further proved its functionality in powering small-scale electronics and a monitoring program that provides real time information on the voltage and status of the harvester network.

I have designed a four-stage charge pump circuit and obtained the perimeters of the strip line, antenna, and impedance matching network through theoretical calculations with Matlab and stimulation with RFsim99.

Our experimental results have proved that our constructed wireless energy harvesters have sensitivity of 2701 V/W under the frequency of 1.05 GHz or work under the frequency range of 0.5 GHz to 2.5 GHz. Two peaks exist within this range: at 0.5 GHz and 2.2 GHz.

I found that the energy harvester can power a thermo hygrometer, proving great potential in real-life applications.

To facilitate its applications in IoT, I have further introduced an in situ wireless voltage monitoring system to obtain information of the harvesters' real time voltages.

This work has developed a solution that utilizes ambient wireless energy to power electronics. It has tested its practicality in applications such as the IoT.

In this work, I have proven wireless energy harvesters' application in networks. Due to our harvester's high conversion efficiency, it has great application in scenarios where alternating current needs to be transformed into direct current, such as nano-generators, rectification circuits, and wireless charging.

In this work, my energy harvester is dual-band. In future works, by introducing multiple antennas or matching circuits, I can achieve even greater bandwidth. I could develop energy collecting metrics to achieve greater output. Overall, I would like our harvester to attain even greater energy output, bandwidth, and sensitivity and industrial applications.

Acknowledgments

Authors wishing to acknowledge assistance or encouragement from colleagues, special work by technical staff or financial support from organizations should do so in an unnumbered Acknowledgments section immediately following the last numbered section of the paper.

References

[1] Portilla, L., Loganathan, K., Faber, H., Eid, A., Hester, J. G. D., Tentzeris, M. M., Fattori, M., Cantatore, E., Jiang, C., Nathan, A., Fiori, G., Ibn-Mohammed, T., Anthopoulos, T. D., & Pecunia, V. (2023). Wirelessly powered large-area electronics for the Internet of Things. *Nature Electronics*, *6* (1), 10 – 17. https: //doi.org/10.1038/s41928-022-00898 - 5.

[2] Mahfoudi, H., Tellache, M., & Takhedmit, H. (2016). A wideband fractal rectenna for energy harvesting applications. *2016 10th European Conference on Antennas and Propagation (EuCAP)*, 1 – 4. https: //doi.org/10.1109/EuCAP.2016.7481960.

[3] Roy, S., Tiang, J.-J., Roslee, M. B., Ahmed, M. T., Kouzani, A. Z., & Mahmud, M. A. P. (2022). Design of a Highly Efficient Wideband Multi-Frequency Ambient RF Energy Harvester. *Sensors*, *22* (2), Article 2. https://doi.org/10.3390/s22020424.

[4] Thosar, P., & Mathur, R. (2020). Design and Development of High Efficiency Rectenna for RF Harvesting. *Materials Today: Proceedings*, *29*, 278–285. https://doi.org/10.1016/j.matpr.2020.07.275.

[5] Zhang, X., Grajal, J., Vazquez-Roy, J. L., Radhakrishna, U., Wang, X., Chern, W., Zhou, L., Lin, Y., Shen, P.-C., Ji, X., Ling, X., Zubair, A., Zhang, Y., Wang, H., Dubey, M., Kong, J., Dresselhaus, M., & Palacios, T. (2019). Two-dimensional MoS2-enabled flexible rectenna for Wi-Fi-band wireless energy harvesting. *Nature*, *566* (7744), 368 – 372. https://doi.org/10.1038/s41586-019-0892-1.

[6] Banerjee, J., & Banerjee, S. (2021). RF Energy Harvesting Circuits and Designs. In N. R. Das & S. Sarkar (Eds.), *Computers and Devices for Communication* (pp. 215 – 221). Springer. https://doi.org/10.1007/978-981-15-8366-7_29.

[7] Tran, L.-G., Cha, H.-K., & Park, W.-T. (2017). RF power harvesting: A review on designing methodologies and applications. Micro and Nano Systems Letters, 5 (1), 14. https: //doi.org/10.1186/s40486 - 017 - 0051 - 0.